

TAPERING SCHEMES FOR FCC-ee

D. Domange*¹, K. Andre, C. Hernalsteens, G. Roy, D. Wollmann, CERN, Geneva, Switzerland
¹ also at Université libre de Bruxelles, Brussels, Belgium

Abstract

The electron-positron Future Circular Collider (FCC-ee) is designed to operate at four beam energies, from 45.6 GeV to 182.5 GeV. At such energy levels, the circulating beam loses a significant fraction of its energy via synchrotron radiation. As a single RF insertion is foreseen in the ring, large closed-orbit shifts featuring a typical sawtooth pattern and optics distortions are induced. This in turn leads to a significant reduction of the dynamic aperture if no mitigation is implemented. The solution is to adapt the fields of the magnets to the local beam energy which is referred to as "tapering". For practical reasons, this field adjustment must be realized for groups of magnets to limit the number of powering circuits. An algorithm has been established to self-consistently compute the tapering strengths of a given scheme, the RF phase required to compensate the energy loss and the required orbit corrections. Tapering scenarios, from coarse schemes to fine grained options are studied with the XSuite tracking code in terms of closed-orbit excursion and optics distortion. The results at the Z-pole (45.6 GeV) and $\bar{t}\bar{t}$ (182.5 GeV) energies are discussed in detail.

INTRODUCTION

In high-energy circular lepton colliders, charged particles lose a significant fraction of their energy via synchrotron radiation. The instantaneous radiated power is given by:

$$P = \frac{2}{3} \frac{e^2}{4\pi\epsilon_0} \frac{\beta^4 \gamma^4}{\rho^2}$$

with e , the elementary charge, ϵ_0 , the vacuum permittivity, β and γ , the relativistic factors and ρ , the local bending radius [1]. The energy offset brings the beam onto a dispersive trajectory which results in a modification of the periodic closed-orbit.

At LEP, as well as with past lepton colliders, studies were conducted to understand the orbit shift at the interaction points caused by energy deviations between the electron and the positron beams [2, 3]. At LEP energies, ranging from 45 GeV to 104.5 GeV, the horizontal closed orbit shift, producing the characteristic sawtooth pattern, had to be compensated. As a distributed RF system was implemented, the cavities could restore the lost energy while minimizing orbit deviations [4, 5].

The 90.66 km-long electron-positron Future Circular Collider (FCC-ee) is expected to operate at four beam energy stages, from 45.6 GeV to 182.5 GeV. Unlike LEP, in the current design, the RF system is located in a single technical insertion of the machine (see Fig. 1) and therefore

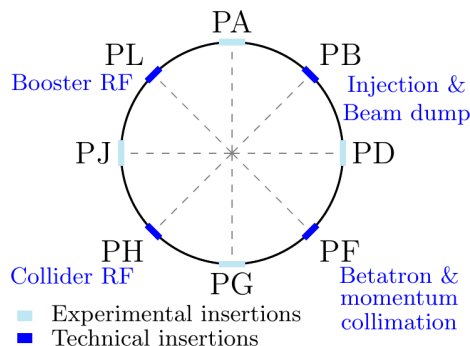


Figure 1: Schematic of the FCC-ee layout. It illustrates the 8 arcs with the 4 experimental insertions and 4 technical insertions. The collider ring RF is located at point PH.

Table 1: FCC-ee Collider Parameters (V24.3 GHC Lattice)

	Z	W	ZH	$\bar{t}\bar{t}$
Beam energy (GeV)	45.6	80	120	182.5
Energy loss / turn (%)	0.039	0.369	1.86	9.94
	0.09	0.47	1.57	5.64
Hor. emittance ϵ_x (nm)	0.70	2.16	0.66	1.51

cannot compensate the large orbit excursion in multiple locations. The main parameters of the current baseline design (V24.3 GHC lattice) relevant to this study are provided in Table 1 [6].

This design leads to a significant sawtooth effect and optics deviations. At Z-pole energy, less than 1‰ of the beam energy is lost in a single turn, leading to a horizontal orbit excursion of up to 0.68 mm as shown in Fig. 2). At $\bar{t}\bar{t}$ energy, 5.64‰ of the total energy is lost in one turn, and the horizontal orbit excursion could reach several centimetres.

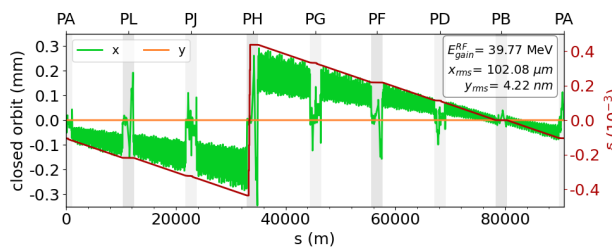


Figure 2: Closed orbit at Z-pole energy with its sawtooth shape for the horizontal plane (green). The sudden change on particle energy deviation δ (red) caused by the energy gain in the RF cavities (PH region), induces the horizontal orbit jump. The vertical closed orbit (orange) is not impacted.

To mitigate the effects of synchrotron radiation, the proposed solution, known as *tapering*, consists of locally adjusting the strength of the magnets to the local beam energy. If each magnet is corrected individually, the resulting configuration is referred to as *ideal tapering*, as it provides the

* delphine.domange@cern.ch

solution closest to the reference closed orbit and optics without synchrotron radiation. For practical reasons, tapering is implemented using average corrections over groups of main magnets (*realistic tapering*) or using orbit correctors, both of which result in closed orbit and optics deviations.

Realistic tapering options can be derived from the powering scheme of the main magnets. As shown in Fig. 1, the collider is divided into eight arcs, each containing two dipole powering circuits and four quadrupole circuits—two focusing and two defocusing. The arc sextupoles are powered in families: 75 at Z-pole and W-pole energies and 146 at ZH and $\bar{t}\bar{t}$ energies [6, 7].

Tapering has been studied for previous FCC-ee layouts, where two RF cavity insertions were considered [8, 9]. This new study compares different realistic tapering schemes for the current design by evaluating their impact on closed orbit excursion, beta beating, dispersion shift, and emittance growth. To enable this analysis, a self-consistent algorithm was developed.

ALGORITHM AND IMPLEMENTATION

Tapering is implemented by adjusting the magnet strengths, which alters the closed orbit. As a result, particles circulate with a different offset in the machine, leading to changes in total energy loss due to synchrotron radiation, and energy deviation within the magnets.

This new algorithm (Fig. 3), developed in XSuite [10], based on closed orbit search, is applied iteratively until both the closed orbit deviation and the total energy loss are minimised. The final configuration corresponds to the fixed point of this optimisation function.

The steps of the algorithm are as follows. Once the initial closed orbit is found, the energy deviation across each element is computed and used to adjust the corresponding magnet strength. The result of these individual corrections corresponds to the ideal tapering. Next, the RF phase (ϕ) is set to compensate for the total energy loss (E_{loss}) using:

$$\phi = \arcsin\left(\frac{E_{loss}}{e V_0}\right)$$

where e is the elementary charge, and V_0 is the RF voltage. A new closed orbit is then computed, and the total energy loss is recalculated. If the difference between the previous total energy loss and the newly calculated is below the set tolerance, or if the maximum number of iterations is reached, the updated lattice is returned.

Additionally, realistic tapering models can be studied. For the specified magnet groups (provided as input), the average correction is computed from individual magnet adjustments, and this single value is applied to the entire group. Magnets not included in any group can either be corrected individually or left uncorrected. For these realistic schemes, the correction is imperfect, resulting in residual orbit deviations. To prevent orbit errors propagation between different magnet groups, an additional local correction is implemented. For dipoles, the last two magnets in each group are used to steer

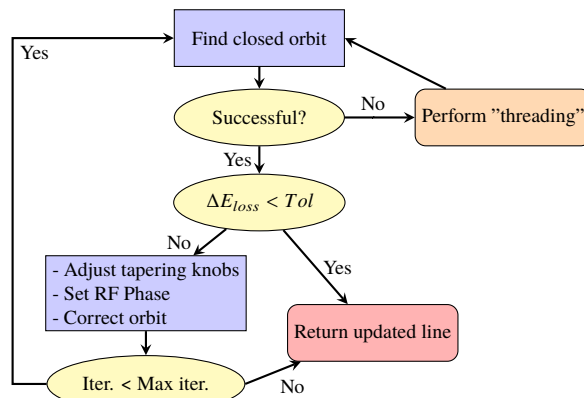


Figure 3: Tapering algorithm.

the orbit back to its reference trajectory. This is performed inside the algorithm loop, as it affects the closed orbit.

To ensure the function is as generic as possible, an additional step can be performed if the initial closed orbit search fails. This may occur if synchrotron radiation effects are too strong or if the model's initial parameters are not adequately pre-set. In such cases, a pre-correction of the lattice—referred to as *threading*—is carried out (shown in orange in Fig. 3). A step-by-step tracking of a single particle is performed. After each magnet, the energy deviation is calculated and used to adjust the magnet strength. The particle is then tracked again through the corrected magnet and the next element. This correction process is repeated over a full turn of the machine. Threading may be executed multiple times before attempting the closed orbit search.

RESULTS

Multiple tapering schemes based on arc magnet groupings have been designed and evaluated. For dipoles and quadrupoles, each of the eight arcs of the machine is divided by a power of two. For example, using 16 groups of quadrupoles corresponds to dividing each arc into two groups, for both focusing and defocusing quadrupoles. For sextupoles, the existing powering circuits can be reused due to the use of single-aperture magnets, and tapering is applied by families. Other magnets are either tapered individually or left uncorrected. The studied models are named according to the following convention:

D	→ Arc dipoles	$\left\{ \begin{array}{l} \# = \text{Individual tapering} \\ \text{Number} = \text{Number of groups} \\ \text{C} = \text{Existing powering circuit} \\ 0 = \text{No tapering} \end{array} \right.$
...		
Q	→ Arc quadrupoles	
...		
S	→ Arc sextupoles	
...		
M	→ All other magnets	
...		

Several of these schemes are listed in Table 2 for both $\bar{t}\bar{t}$ and Z-pole energies. Focusing on $\bar{t}\bar{t}$ energy—where tapering has a more significant impact—the effect of grouping granularity for each type of magnet can be analysed. To compare the models, their deviation from the ideally tapered lattice is quantified using the following parameters: horizontal RMS closed orbit (x_{rms}), RMS beta beating ($\Delta\beta/\beta_{ref}$),

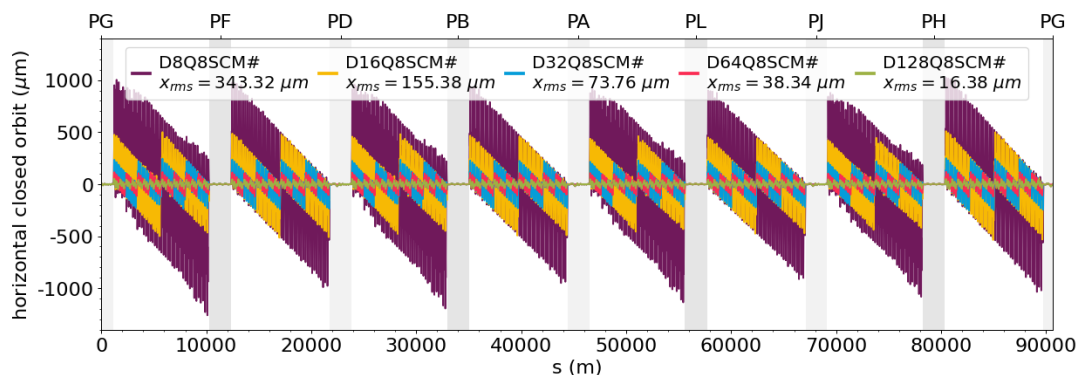


Figure 4: Comparison of different realistic tapering schemes at $t\bar{T}$ energy. The horizontal closed orbit is represented for each grouping granularity of the arc dipoles (8 to 128 groups). The finer the division, the smaller the orbit deviation. The orbit is brought back to the reference at the end of each group to avoid error propagation.

Table 2: Comparison of different tapering schemes for $t\bar{T}$ (lines 1-10) and Z-pole (lines 11-12) energies. The reference is the ideally tapered lattice. For the beta beating and the dispersion shift, the RMS value is given.

Tapering scheme	x_{rms} (μm)	$\frac{\Delta\beta_x}{\beta_{xref}}$ (%)	$\Delta\eta_x$ (mm)	$\frac{\Delta\epsilon_x}{\epsilon_{xref}}$ (%)
1 D8Q8SCM#	341.66	155.79	31.13	105.40
2 D16Q8SCM#	155.76	56.55	17.578	23.11
3 D32Q8SCM#	73.79	37.88	4.97	9.77
4 D64Q0SCM#	39.70	11.16	34.73	9.44
5 D64Q8SCM#	38.34	7.47	3.07	0.46
6 D64Q16S0M#	38.34	10.70	2.55	0.75
7 D64Q16SCM#	38.34	10.71	2.55	0.75
8 D64Q16S#M#	38.34	10.71	2.55	0.75
9 D64Q32SCM#	38.34	8.11	2.50	0.45
10 D128Q8SCM#	16.38	3.69	1.57	0.05
11 D8Q8SCM#	17.54	2.15	2.1	0.06
12 D128Q8SCM#	1.22	0.04	0.31	-0.01

RMS horizontal dispersion shift ($\Delta\eta$) and relative horizontal emittance growth ($\Delta\epsilon_x/\epsilon_{ref}$). Each lattice is rematched to the design tune prior to comparison.

Dipole tapering plays a major role. When comparing different granularity for arc dipoles (from 8 to 128 groups), the impact on closed orbit deviation is clearly visible in Fig. 4 and Table 2 (highlighted in green). The finer the granularity, the smaller the orbit deviation. To limit orbit excursions to a few micrometers—within the range of an orbit correction system—128 groups are required (Table 2, line 10). In this configuration, the beta beating, the dispersion shift and the emittance growth are limited and remain within acceptable operational limits [11, 12].

Grouping of the other arc magnets has more indirect effects, primarily visible in optic deviations rather than direct orbit distortion. Comparison of different groupings for quadrupoles (Table 2, lines 4, 5, 7 and 9) show that a minimum of 8 quadrupole groups is sufficient to effectively control optics deviations, particularly emittance growth (highlighted in blue), which is critical for maintaining high lu-

minosity. The optics perturbations induced by the tapering scheme must be limited in a range compatible with the foreseen optics correction and tuning capabilities. Tapering of sextupoles has limited overall impact (Table 2, lines 7-9) but does not induce additional cost.

In conclusion, the scheme D128Q8SCM# is a good realistic tapering scheme for FCC-ee operation at $t\bar{T}$ energy. Implementing this model would require at least 144 new power converters per beam (128 for dipoles and 2×8 for quadrupoles). Since both dipoles and quadrupoles are twin-aperture magnets, additional coils must be used, as the required corrections are opposite for each side of the machine.

At Z-pole energy, the same conclusions regarding the effect of magnet grouping granularity remain valid. Since synchrotron radiation scales with particle energy, the D8Q8SCM# scheme (Table 2, line 11) yields results comparable to D128Q8SCM# at $t\bar{T}$ energy. Nevertheless, as the design strategy aims to reuse the same hardware across all operational modes, a unified tapering scheme is preferred. This configuration performs very well at Z-pole energy (Table 2, line 12).

CONCLUSION

In FCC-ee, particles will undergo significant energy loss due to synchrotron radiation, resulting in orbit deviations and optics errors that degrade overall machine performance. Mitigating these effects is essential, and tapering is one of the proposed solutions. The developed algorithm determines, in a self-consistent manner, the corrections to be applied to the magnets, either individually or by group, as well as the required RF phase advance. This study demonstrates that the tapering of arc dipoles is the primary factor influencing tapering performances. Optics deviation can be limited with a coarse tapering of the quadrupoles. 128 groups of dipoles and 8 groups of quadrupoles are required at $t\bar{T}$ energy for efficient tapering. Further studies evaluating the overall machine performance mainly in respect to dynamic aperture and luminosity need to be performed. The proposed algorithm has been designed to be compatible with such analyses.

REFERENCES

- [1] R. P. Walker, “Synchrotron radiation”, in *CAS - CERN Accelerator School: 5th General Accelerator Physics Course*, Jyväskylä, Finland, Sep. 1992, pp. 437-459. doi:10.5170/CERN-1994-001.437
- [2] M. J. Lee, P. L. Morton, J. R. Rees, and B. Richter, “Control of closed orbit deviation due to synchrotron radiation”, *IEEE Transactions on Nuclear Science*, vol. 22, no. 3, pp. 1914-1915, 1975. doi:10.1109/TNS.1975.4328026
- [3] J.-P. Koutchouk, “The horizontal closed orbit of a radiating beam”, CERN, Geneva, Switzerland, CERN-LEP-Note-578, 1987. <https://cds.cern.ch/record/443003>
- [4] M. Bassetti, “Effects due to the discontinuous replacement of radiated energy in an electron storage ring”, in *11th Int. Conf. on High-Energy Accelerators*, Geneva, Switzerland, Jul. 1980, pp. 650-655. doi:10.1007/978-3-0348-5540-2_89.
- [5] C. Wyss, “LEP design report, v.3: LEP2”, CERN, Geneva, Switzerland, CERN-AC-96-01-LEP-2, 1996. <http://cds.cern.ch/record/314187>
- [6] M. Benedikt, F. Zimmermann, *et al.*, “Future Circular Collider Feasibility Study Report Volume 2: Accelerators, technical infrastructure and safety”, CERN, Geneva, Switzerland, CERN-FCC-ACC-2025-004, 2025. doi:10.17181/CERN.EBAY.7W4X
- [7] FCC-ee lattice GitLab repository, V24.3_GHC baseline. <https://gitlab.cern.ch/acc-models/fcc/fcc-ee-lattice>
- [8] B. Härer, A. Doblhammer, and B. Holzer, “Tapering Options and Emittance Fine Tuning for the FCC-ee Collider”, in *Proc. IPAC’16*, Busan, Korea, May 2016, pp. 3767-3770. doi:10.18429/JACoW-IPAC2016-THPOR003
- [9] M. Racic, “Modeling alternative tapering schemes for electron-positron Future Circular Collider (FCC-ee)”, Master thesis, EPFL, Lausanne, Switzerland, 2021.
- [10] G. Iadarola, R. De Maria, S. Łopaciuk, A. Abramov, *et al.*, “Xsuite: An Integrated Beam Physics Simulation Framework”, in *Proc. HB’23*, Geneva, Switzerland, Oct. 2023, pp. 73-80. doi:10.18429/JACoW-HB2023-TUA2I1
- [11] T. K. Charles, B. Holzer, R. Tomas, K. Oide, *et al.*, “Alignment & stability challenges for FCC-ee”, in *EPJ Tech. Instrum.*, vol. 10, no. 1, p. 8, 2023. doi:10.1140/epjti/s40485-023-00096-3
- [12] E. Musa, I. Agapov, and T. Charles, “Orbit-response based optics corrections for FCC-ee”, in *Proc. IPAC’23*, Venice, Italy, May 2023, pp. 3143-3146. doi:10.18429/JACoW-IPAC2023-WEPL017